

UNCLASSIFIED

AD 402 328

*Reproduced
by the*

DEFENSE DOCUMENTATION CENTER

FOR

SCIENTIFIC AND TECHNICAL INFORMATION

CAMERON STATION, ALEXANDRIA, VIRGINIA



UNCLASSIFIED

NOTICE: When government or other drawings, specifications or other data are used for any purpose other than in connection with a definitely related government procurement operation, the U. S. Government thereby incurs no responsibility, nor any obligation whatsoever; and the fact that the Government may have formulated, furnished, or in any way supplied the said drawings, specifications, or other data is not to be regarded by implication or otherwise as in any manner licensing the holder or any other person or corporation, or conveying any rights or permission to manufacture, use or sell any patented invention that may in any way be related thereto.

63-3-2

AFCL - 63 - 284

402328

CATALOGED BY ASTIA
AS AD NO. _____

402 328

ASTIA
RECEIVED
APR 30 1963
TISIA

Monitoring Agency Document Nr.:

ASTIA Document Nr.:

SOME PROBLEMS OF ATMOSPHERIC DIFFUSION
ON VERY LARGE SCALE

F. MESINGER

INSTITUT FÜR METEOROLOGIE
TECHNISCHE HOCHSCHULE DARMSTADT
DARMSTADT, FED. REP. OF GERMANY

TECHNICAL NOTE NR. 2
CONTRACT NR.: AF 61 (052)-366

31st OCTOBER 1962

The research reported in this document has been sponsored partly by the CAMBRIDGE RESEARCH LABORATORIES, OAR, through the European Office Aerospace Research, United States Air Force.

SOME PROBLEMS OF ATMOSPHERIC DIFFUSION
ON VERY LARGE SCALE

By F. Mesinger +)

Abstract

Making use of a 500 mb numerical forecast some problems of atmospheric large-scale diffusion are investigated. The expansion of various sets of clusters of particles is compared with the predictions based on the similarity theory of homogeneous turbulence. The spreading rates were in the beginning of the period of the forecast in a good agreement with the theoretical predictions, but later on they dropped to values considerably smaller than the predicted ones. The reasons of such a behaviour are discussed. Furthermore the difference in zonal and meridional expansions of the clusters is demonstrated; the zonal expansion rates are more than one order of magnitude greater than the meridional ones.

The intrinsic property of turbulence to disturb initially equidistantly spaced particles until the random distribution is achieved is investigated with respect to its time scale. It is found that the atmosphere needs about 6 days to move the initially rectangularly spaced particles 381 km apart to the positions which form the distribution differing 10 per cent from the random distribution.

1. Introduction

It was only comparatively recently that in diffusion studies the proper attention has been paid to the difference between the diffusion from a fixed source and the diffusion relative to a moving origin of a single puff or cluster of particles.

+) Technische Hochschule Darmstadt, Department of Meteorology;
on leave from University of Beograd, Jugoslavia

The former diffusion type was first analysed by G.I. Taylor in the well known paper in 1921. The latter type was discussed by L.F. Richardson already in 1926, but it was not before about 1950 that in several basic studies by Brier and Batchelor the detailed mathematical analysis of the problem was given. Also a lot of experimental work has been devoted to both diffusion problems. The main achievements along all these lines are comprehensively reviewed in a recent study by Pasquill (1962).

Various experimental investigations cover the whole range of diffusion processes which are experienced in the atmosphere, up to the diffusion on the largest i.e. synoptic scale. Here on this synoptic-scale diffusion process our attention will be fixed. A description of the diffusion on the synoptic scale can be achieved in a direct way by the observations of the trajectories of some markers floating in the air (constant-level balloons for instance). An alternative procedure is to compute air trajectories in some way. In previous investigations of this sort (Durst et al., 1959) the interest was concentrated mainly in the dispersion of the end-points of air trajectories initiated at regular intervals at a fixed point (fixed-source diffusion type). In this paper some information concerning the complementary problem of relative diffusion of clusters of particles will be presented.

The ideal way of studying the expansion of a given large-scale cluster is to know the trajectories of individual particles of the cluster. To this end the use of constant-level balloons data can, because of the sparsity of balloon flights in space, hardly be made. Particle trajectories can be computed from successive contour maps with the use of geostrophic, as in the work by Durst et al., or some other wind approximation. In our study the particle trajectories were obtained by the application of a numerical weather prediction procedure. The main reason for this choice lied in computation facilities, since the numerical prediction program, suitable for the computation of a large number of

trajectories, was available for the investigation purposes. The use of the "forecast" instead of the "hindcast" trajectories brings in the diffusion results systematic errors inherent in the adopted forecasting model (steady decrease in eddy kinetic energy), and this must be borne in mind at the examination of the computation results.

The large number of computed trajectory coordinates suggested furthermore the idea to study the time scale of the tendency of turbulence to move initially regularly spaced particles to the positions for which the initial spacing is completely disturbed and the random distribution is achieved. A discussion of this problem is given in section 4. As an indication of this process the mean value and the frequency function of the distance from every particle to the particle nearest were taken.

2. Computations of the cluster-expansion rates

Trajectory computations were based on the integration of the set of primitive equations

$$\begin{aligned}\frac{\partial u}{\partial t} &= m^2(-\mathbf{w} \cdot \nabla u + \nabla^2 u) - \frac{u^2 + v^2}{2} \frac{\partial m^2}{\partial x} + fv - \frac{\partial \phi}{\partial x}, \\ \frac{\partial v}{\partial t} &= m^2(-\mathbf{w} \cdot \nabla v + \nabla^2 v) - \frac{u^2 + v^2}{2} \frac{\partial m^2}{\partial y} - fu - \frac{\partial \phi}{\partial y}, \\ \frac{\partial \phi}{\partial t} &= -m^2 \nabla \cdot (\phi \mathbf{w}),\end{aligned}\quad (1)$$

valid for the homogeneous atmosphere (Hollmann, 1959). In (1) x and y are the Cartesian coordinates of the image surface of stereographic projection, $\mathbf{w}(u, v)$ is the so called "reduced image velocity" (Hollmann, 1959), while other

symbols have their conventional meanings. Some details of the computation procedure are already described elsewhere (Mesinger, 1962).

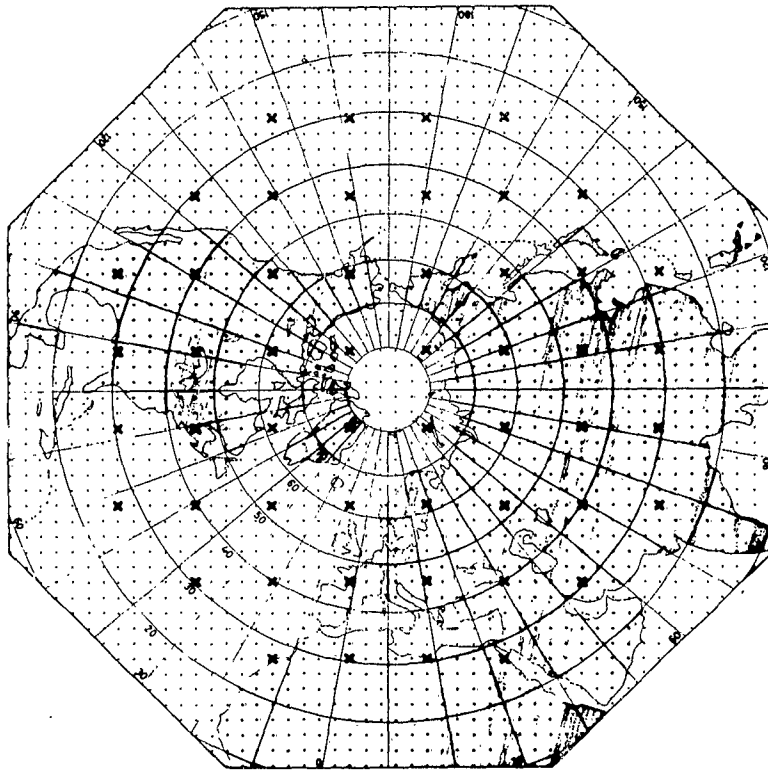


Fig. 1. Grid. Horizontal grid distance 381 km in the image surface of stereographic projection, crossing the earth's surface at 60°N . Grid points indicated by crosses are centers of the clusters at the beginning of the forecast.

The program available for the solving of system (1) on an IBM 704 computer was designed for the grid consisting of 2080 points evenly spaced on an octagonal area centered on the North Pole. With the adopted grid distance of 381 km

at 60°N latitude the computation area extended southward to about 10°N latitude (Fig. 1). Starting with the geopotential field of the 500 mb surface for the 00 GMT 26 August 1958, shown in Fig. 2, a forecast for the period of 8 days was made. On this occasion the kinematic eddy-viscosity coefficient ν in (1) the value of $0.517 \cdot 10^9 \text{ cm}^2 \text{ sec}^{-1}$ was prescribed (round number in binary system). There is some evidence that this could be about the right value for the grid size used in the computations (Phillips, 1956, p.131).

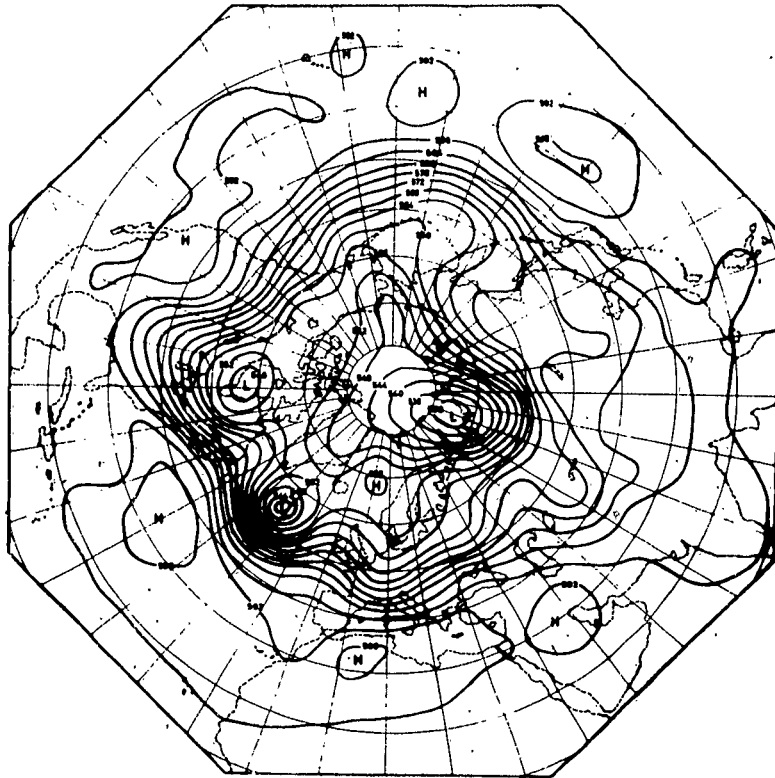


Fig. 2. The initial situation: contour height of the 500mb surface, for the 00 GMT 26 August 1958.

Making use of successive wind fields at intervals of half an hour, obtained as an output of this 8-day forecast,

the trajectories were computed for all the 2080 particles situated at the beginning of the forecasting period in the grid points. This was done with the formulae centered in time and space. Fields of particle coordinates at one-hour time intervals were written on magnetic tapes as an output of the trajectory computation program. Particles were then combined in suitable sets to form various clusters. There were 52 clusters of each sort, having their centers at the beginning of the forecasting period at 52 grid points evenly distributed over the computation area (Fig. 1). Out of the tapes with the particle coordinates mean standard deviations of the particles about the gravity centers of the clusters (σ 's) were evaluated at time intervals of 6 hours. This was done with the aid of two programs:

(a) A program evaluating standard deviations for three sorts of square-formed clusters, consisting of 3×3 , 5×5 and 7×7 particles, respectively.

(b) A program evaluating standard deviations separately in zonal and meridional directions for five sorts of diamond-formed clusters, consisting only of 4 particles at 1, 2, 3, 4 and 5 grid distances away from the center, respectively.

Since some other research on atmospheric macroturbulence was carried on parallel with these computations, several statistical quantities useful for the interpretation of the cluster-expansion results were available for this purpose.

3. Discussion of the computed cluster-expansion rates

Regarding the rates of expansion of the clusters, the most interesting point is how far they agree with the Batchelor's predictions (Batchelor, 1950) based on the similarity theory of homogeneous turbulence. Assuming that the cluster size is small compared to the size of the energy-containing eddies (an assumption which seems to be fulfilled at least for the smallest 9-point clusters) Batchelor arrives at the

relations

$$\sigma^2 - \sigma_0^2 \propto t^2 \quad (\text{small } t), \quad (2)$$

and

$$\sigma^2 \propto t^3 \quad (\text{intermediate } t), \quad (3)$$

where the distinction between "small" and "intermediate" times is given approximately by the value

$$t_1 = \sigma_0^{2/3} \epsilon^{-1/3} \quad (4)$$

Here ϵ represents the average rate of dissipation of eddy kinetic energy. Relation (3) should apply to the clusters whose expansion is already independent of the initial cluster size, but is still governed by the eddying motions belonging to the inertial subrange of eddy sizes. These formulae of Batchelor were tested by Gifford (1957a, 1957b) on the basis of various sets of smoke-puff spreading data. He concluded that the existence of the predicted t^2 and t^3 regimes for the growth of small puffs seems to be strongly supported by the experiments.

To check the applicability of the relations (2) and (3) to our large-scale cluster data values of $\sigma^2 - \sigma_0^2$ and σ^2 obtained with the program (a) were plotted vs. t on a logarithmic paper (Fig. 3). Assumption of the law $\sigma^2 - \sigma_0^2 \propto t^\alpha$ gives for the exponent α values ranging for small times from 1.95 to 2.05; so Rel. (2) represents an excellent fit to the data. An equivalent assumption for σ^2 gives for the exponent α at the most values ranging from 1.40 to 1.60. These values are reached at times of 6-8 days, and the inspection of the trend of the curves does not give an indication that the exponents could attain significantly greater values at the later times. Moreover, exponent values should decrease afterwards, since in the limiting case of very large t , when the whole energy-spectrum is effective, cluster must behave in functionally the same way as the plume, i.e. exponent values

should tend to unity.

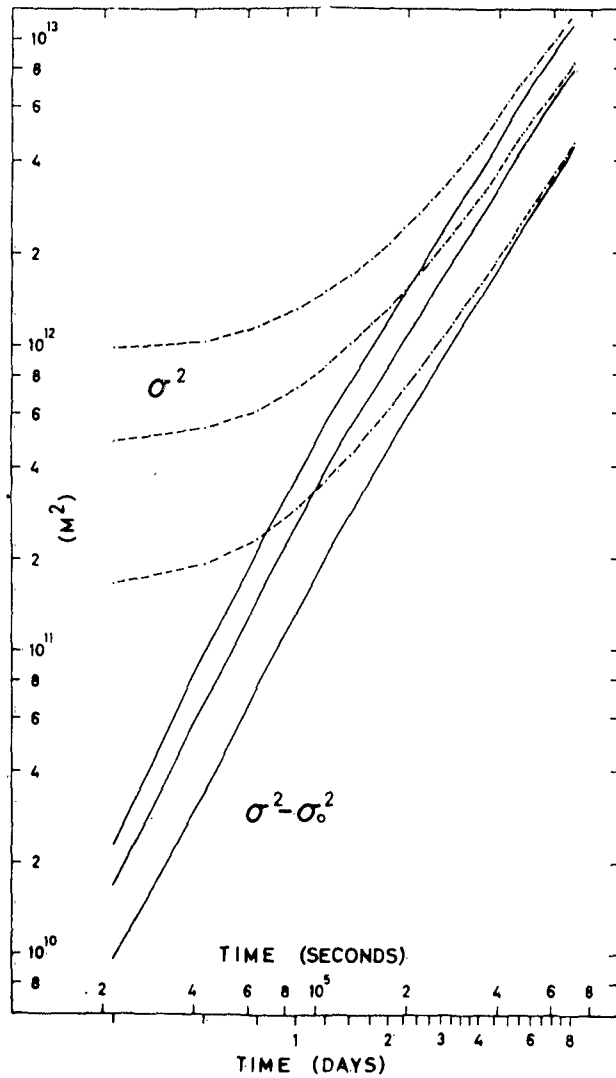


Fig. 3. Mean-square particle dispersion (dashed lines), and increase of mean-square particle dispersion relative to its initial value (full lines), for three sorts of initially square-formed clusters. Clusters consisted of 9, 25 and 49 particles, with initial standard deviations about the gravity centers of 393, 681 and 964 km respectively.

Here the question arises whether the 8-day period is long enough to include the time t_1 , after which the t^3 regime should be expected. To evaluate t_1 we must know the value of ϵ , but not much is known about the right values of ϵ in the atmosphere. Since in scope of our investigations also a 4-day computation without the energy-dissipation term in (1) was made, an estimate of ϵ can be made from the difference in eddy kinetic energies of the two computations (Fig. 4). During 4 days the eddy kinetic energy (mean value over the whole computation area) of the 8-day forecast, due to the influence of the energy-dissipation term, decreased for $1.32 \text{ m}^2 \text{ sec}^{-2}$ compared to that of the 4-day forecast. This gives for the energy dissipation

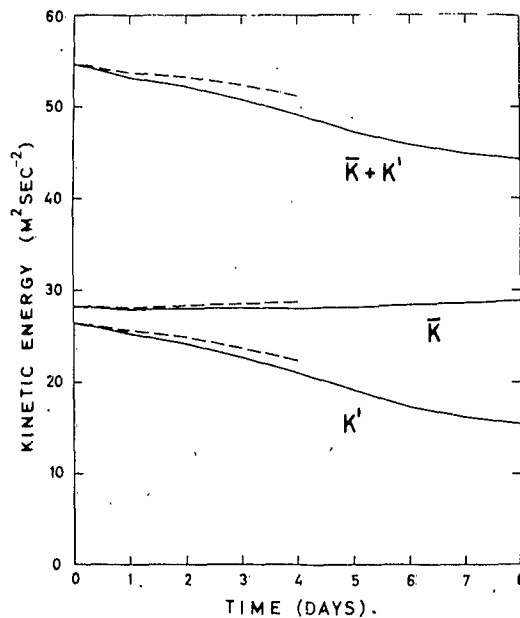


Fig. 4. Kinetic energies of the perturbed motion (K'), mean motion (\bar{K}), and their sum, as functions of time. Dashed lines are the result of the forecast made without the energy-dissipation term in Eqs. (1), and full lines are the result of the forecast made with the value $\nu = 0.517 \cdot 10^9 \text{ cm}^2 \text{ sec}^{-1}$ in (1).

rate the value of $0.038 \text{ cm}^2 \text{ sec}^{-3}$. It is interesting that this value fits well in with the trend in variation with height of several estimates of ϵ obtained from the small-scale diffusion experiments (Pasquill, 1962, p.161). Application of the value of $0.038 \text{ cm}^2 \text{ sec}^{-3}$ for ϵ gives for the time t_1 values ranging from 4.0 days (9-point clusters) to 7.2 days (49-point clusters); this supports the idea that the time t_1 is included in the time scale of Fig. 3.

The failure of Fig. 3 to show the existence of the t^3 regime should not be considered as a proof of inapplicability of the simplifications of inertial subrange to the large-scale atmospheric diffusion. We must take into account that the forecast underlying the cluster-expansion computations showed a steady decrease in eddy kinetic energy (Fig. 4), amounted after the 8 days to 41 per cent of the initial value. This loss in eddy kinetic energy was due to the (a) truncation in time and space, (b) transformation of eddy kinetic energy into the kinetic energy of the zonally averaged motion, and (c) dissipation of eddy kinetic energy; the dissipation was expected to differ from its natural value with respect to the adopted viscosity coefficient. In real atmospheric stream fields the loss under the item (a) does not exist, and the losses under the items (b) and (c) are in the average compensated by the transformation of eddy potential energy into eddy kinetic energy. Hence, in real atmospheric stream fields we must expect cluster-expansion rates to be greater to a certain extent. This implies that the initial expansion rates, found to be in a good agreement with the Rel.(2), should also be greater.

Furthermore we must have in mind that in our case an upper limit of the size of the clusters exists, in contrary to the considerations which led to the prediction (3). The approaching to that limit could also at least partly be the reason of the lacking of the t^3 regime.

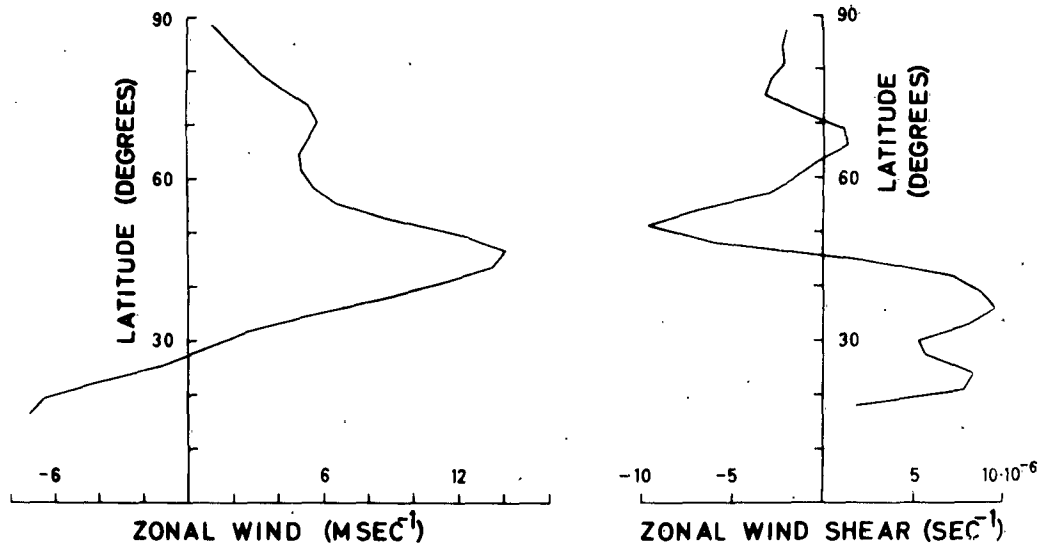


Fig. 5. Zonally averaged wind, and its shear, of the initial situation shown in Fig. 2.

In theoretical investigations of relative diffusion the influence of the shear of the mean flow is not taken into account. Having in mind the idea to study this influence experimentally, in scope of the program (a) mean standard deviations were computed separately for the 40 clusters south of the 57°N latitude, where the amount of shear of the mean flow was comparatively great, and for the 12 clusters north of the 57°N latitude, where the amount of shear was small (Fig. 5). The results of this separation are shown in Fig. 6. Clusters south of the 57°N had greater spreading rates than those north of the 57°N, the difference being greater for clusters of larger initial size. But since in regions south of the 57°N also the eddy kinetic energy was to some extent greater than north of the 57°N (Fig. 7), it is hard to say

how much the greater spreading rates south of the 57°N were a consequence of the greater zonal wind shear.

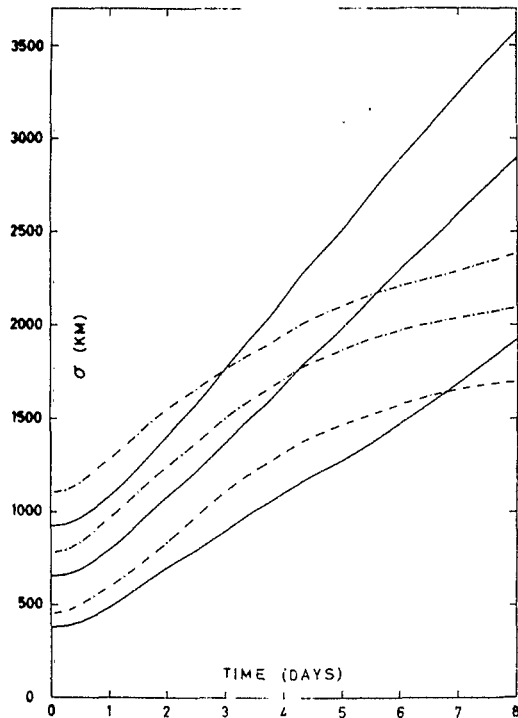


Fig. 6. Mean standard deviations of the 40 clusters initially situated south of the 57°N (full lines), and of the 12 clusters initially situated north of the 57°N (dot-dashed lines). Difference in the initial sizes is due to the increase in grid distance with latitude.

In computations with the program (b) only the 40 clusters south of the 57°N were included, since in polar regions the evaluation of zonal and meridional distances with sufficient accuracy becomes complicated and sometimes senseless. The number of particles in the clusters was restricted to only 4 because of the great consumption of time for the automatic computation of mean longitude for clusters consisting of

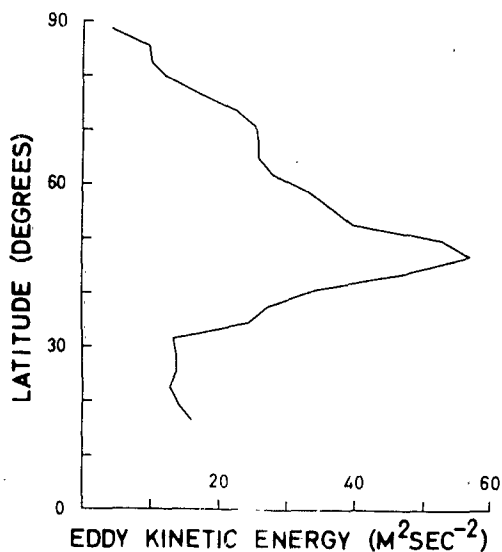


Fig. 7. Eddy kinetic energy of the initial situation shown in Fig. 2.

a great number of particles. Results, shown in Fig. 8, give for the zonal spreading rates values more than one order of magnitude greater than for the meridional ones. It has already been described (Welander, 1955; Djurić, 1961) that the atmospheric diffusion has a property to elongate fluid surfaces into long and thin bands. As shown by this computation these bands have a strong tendency for an east-west orientation. We must however mention that this tendency is somewhat exaggerated in Fig. 8, since the loss in eddy kinetic energy, due to deficiencies of the computation model, was much greater for the meridional motion than for the zonal one. The losses in eddy kinetic energies of the meridional and the zonal motion amounted after the 8 days to 66 and 19 per cent of their initial values respectively.

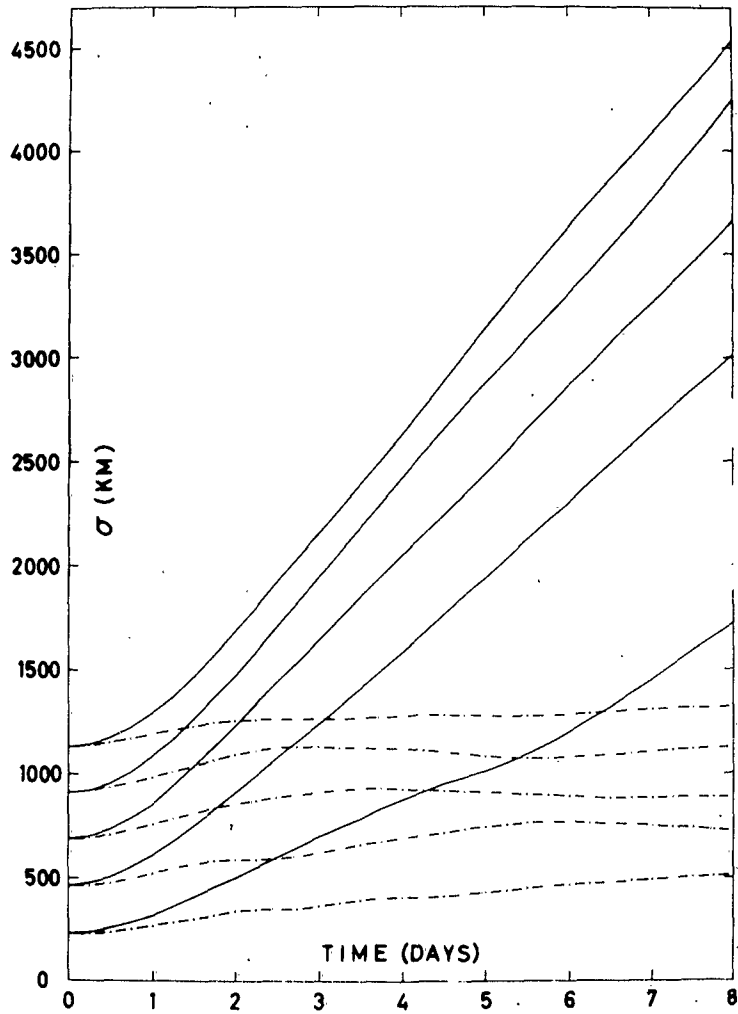


Fig. 8. Mean standard deviations in zonal (full lines) and in meridional (dot-dashed lines) direction, for five sorts of initially diamond-formed clusters.

The tendency for predominantly zonal stretching of the clusters is further illustrated by the Fig. 9, in which the

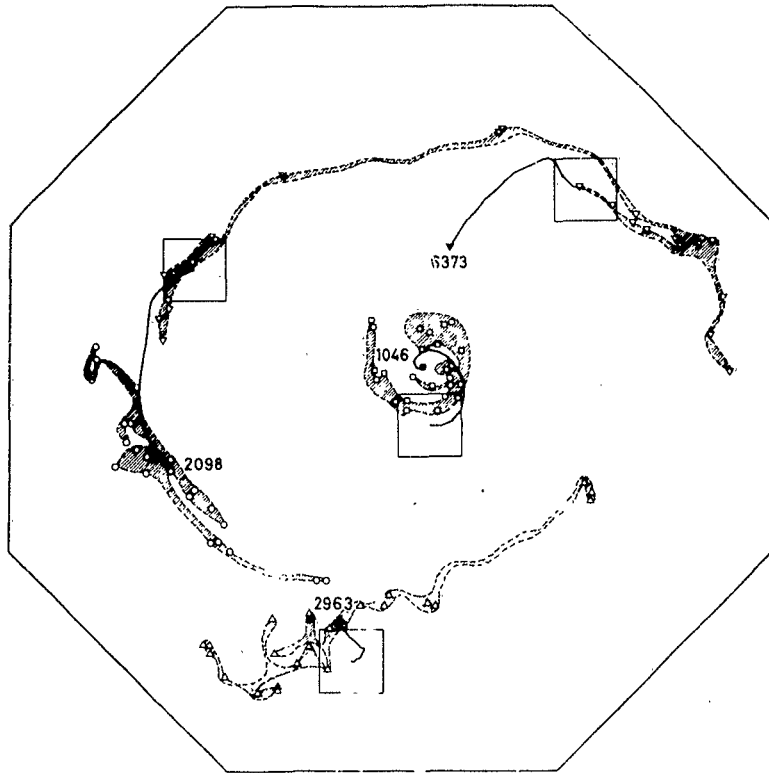


Fig. 9. Shape of 4 selected 25-point clusters after the 8-day period. Same geometrical signs denote the 25 particles of a particular cluster; full sign of the same form denotes their gravity center. Four squares represent the initial positions of the clusters, and shaded areas their approximate 8-day positions. Full lines are the trajectories of the gravity centers of the 4 clusters, and numbers at their ends are the 8-day standard deviations (in kilometers) of the particles of the clusters. The region covered is the same as in Figs. 1 and 2.

form of selected 25-point clusters after the 8-day period is demonstrated. To make an objective choice of the clusters to be demonstrated in Fig. 9 all the 52 25-point clusters

(being intermediate to the other two cluster sizes) were arranged according to their 8-day standard deviation values, and 4 clusters having equidistant positions in this array and at the same time including the extreme two clusters were chosen (1st, 18th, 35th and 52nd cluster). The inspection of the shape and orientation of the clusters shown in Fig. 9, particularly that of the uppermost one with the greatest 8-day standard deviation value, shows that, at least in our computation, the upper limit to the cluster sizes is put rather by this zonal stretching of the clusters than by the finite boundary of the computation area. For a particular cluster this limit is practically reached when it completes a zonal circle, and its center is placed in the vicinity of the pole.

This effect of approaching to the upper limit must evidently influence mostly the greatest clusters. Therefore, in order to investigate to what extent this effect could be responsible for the lack of the t^3 regime, for every sort of square-formed clusters three clusters with greatest 8-day sizes were chosen, and their mean σ^2 -values calculated. The results of this calculation are shown in Table 1.

Table 1. Exponent values of the assumption $\sigma^2 \propto t^\alpha$

Cluster type	3-greatest-clusters exponents at days							max. exponent in considering all the 52 clusters
	1-2	2-3	3-4	4-5	5-6	6-7	7-8	
7>>7	1.20	1.70	1.85	1.80	1.95	1.90	1.90	1.40
5>>5	1.25	2.00	2.30	1.90	1.95	1.80	2.00	1.45
3>>3	1.65	2.50	2.50	2.20	2.25	2.00	2.05	1.60

The exponents of these greatest clusters of any type reach their maximum values somewhat earlier than the exponents of all the 52 clusters together (Fig. 3). Later on the exponents of the greatest clusters decrease a little, nevertheless remaining much greater than the maximum values of the exponent of all the 52 clusters. One gets the impression that the effect of

approaching the upper limit is not significant for the failure of the computation to show the t^3 spreading regime.

4. On a characteristic time scale of turbulence

It is the turbulent character of the motion which gives rise to continuous change of the positions of moving particles relative to each other. Thus when a set of regularly spaced particles is put into a turbulent motion, after a certain time the initial spacing will not more be recognizable. An example of such a situation is given in Fig. 1 of the already cited note of the author (Mesinger, 1962), where the 2080 end points of our 8-days trajectories are demonstrated. In the interior of the computation area no sign of regularity can be seen, and the particles seem to be distributed entirely at random. So the questions arise (a) at what rate will initially regularly spaced air particles under the action of atmospheric motions approach to the state of random distribution, (b) will the atmospheric motions realize such a distribution, and (c) if they do so how much time do they need for that? The time-scale of this process is evidently dependent on the initial distance of the particles, but for a given initial distance it is determined by the intensity of turbulent motions. Hence, this time-scale is an interesting characteristic of the turbulence.

In trying to answer these questions we must first find how to determine to what extent a given distribution of some points coincides with the random distribution. A suitable tool for this determination seems to be the frequency function of the distance from every particle to the particle nearest to it. These "smallest distances", being for the square grid of points all equal to the grid size, must have a definite frequency function when the points are distributed at random. Therefore our next task will be to derive the analytic expression of this frequency function.

To this end consider two concentric circles, and let the areas enclosed by the greater circle and by the smaller one be A and $r^2\pi$ respectively. Now when N points are placed at random in the greater circle, the probability that no one of them will fall in the smaller one is equal to $(1 - r^2\pi/A)^N$. The probability of the complementary event that at least one point will fall in the smaller circle is

$$1 - (1 - r^2\pi/A)^N . \quad (5)$$

When we are dealing with a great number of points distributed over a relatively large area it is suitable to drop out of consideration the influence of the finite boundary of the area A . Hence we allow N and A to tend to infinity, keeping at the same time the average number of points per unit area $n = N/A$ constant. The expression (5) then goes over to

$$1 - e^{-n\pi r^2} , \quad (6)$$

and has moreover become independent of the position of the center of the "smaller" circle. Thus we can imagine this circle centered on any one of the points considered, and (6) will then represent the probability $P(d < r)$ that the distance d to the point nearest of it takes a value smaller than the radius of the circle r . In other words (6) is equal to the distribution function of d , and its first derivative

$$f(r) = 2n\pi r e^{-n\pi r^2} \quad (7)$$

is the desired frequency function of the random variable d .

It is also of interest to know the mean value of the variable d , and the mode of its distribution. Mean value is equal to the first moment of the distribution,

$$\bar{d} = \int_0^{\infty} r f(r) dr , \quad (8)$$

or according to (7),

$$\bar{d} = 1/2n^{1/2} . \quad (9)$$

Mode of the distribution of d is equal to

$$r_m = (2n\pi)^{-1/2}. \quad (10)$$

For this value of r the frequency function (7) takes its maximum value

$$f(r_m) = (2n\pi/e)^{1/2}. \quad (11)$$

For a given average density of points it is convenient to choose the unit of length so to have $n = 1$. Then we have from (9), (10) and (11) $\bar{d} = 0.5$, $r_m = 0.3989$ and $f(r_m) = 1.520$, respectively. Thus, when points making initially a square grid are brought to the random distribution, the mean and the most frequent distances from every point to the point nearest to it amount to 0.5 and 0.3989 grid sizes, respectively.

On the basis of the forecast described in section 2 a computation was made with the purpose to investigate the process of approaching to the now described random state. The values of d at intervals of 12 hours were computed for all the 970 particles situated at the beginning of the forecast in grid points of the interior of the left half of the grid. On this occasion the change in grid distance, due to change in latitude, was neglected. The choice of the particle nearest to a particular one out of these 970 particles was of course made taking into account distances to all the 2079 remaining particles.

Mean values of so computed distances are shown in Fig. 10. They can be taken as a rough indicator of the randomness of the distribution. Thus we come to the conclusion that the atmospheric motions need about 6 days to realize a distribution differing 10 per cent from the random one, when the initial distance between particles is equal to 381 km. The distribution seems to approach asymptotically to the random distribution. The rate of this approaching is less than the exponential one; this can readily be seen by trying to find an exponential

fit to the curve in Fig. 10. Better fit to the curve in Fig. 10 can be realized by the function of the form

$$d = 0.5 + 0.5(1 + t/a)^{-b} , \quad (12)$$

where the appropriate value of b is about 2.

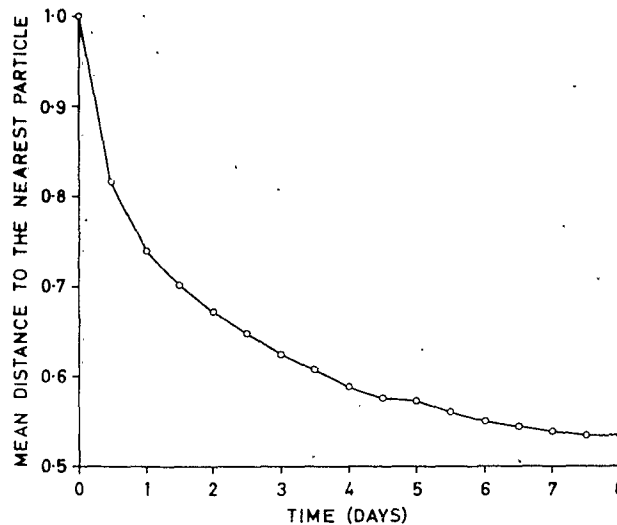


Fig. 10. Mean value of distances from every particle initially situated in a grid point to the other such particle nearest to it, as function of time. The unit of length chosen is the grid size of Fig. 1.

Histograms of the computed distances at time intervals of 2 days, and the frequency curve of the random distribution, given by Eq. (7), are shown in Fig. 11. The agreement of computed histogram with the shape of (7) is fairly good after the 8 days, especially on the decreasing side of the frequency curve. Computed height of the first class interval is at that time greater than the theoretical one after (7) because of the accumulation of particles at the ends of the rows nearest to the boundaries of the area (Mesinger, 1962). The random state would be approached more quickly without the loss of

eddy kinetic energy by the mechanisms described in the preceding section.

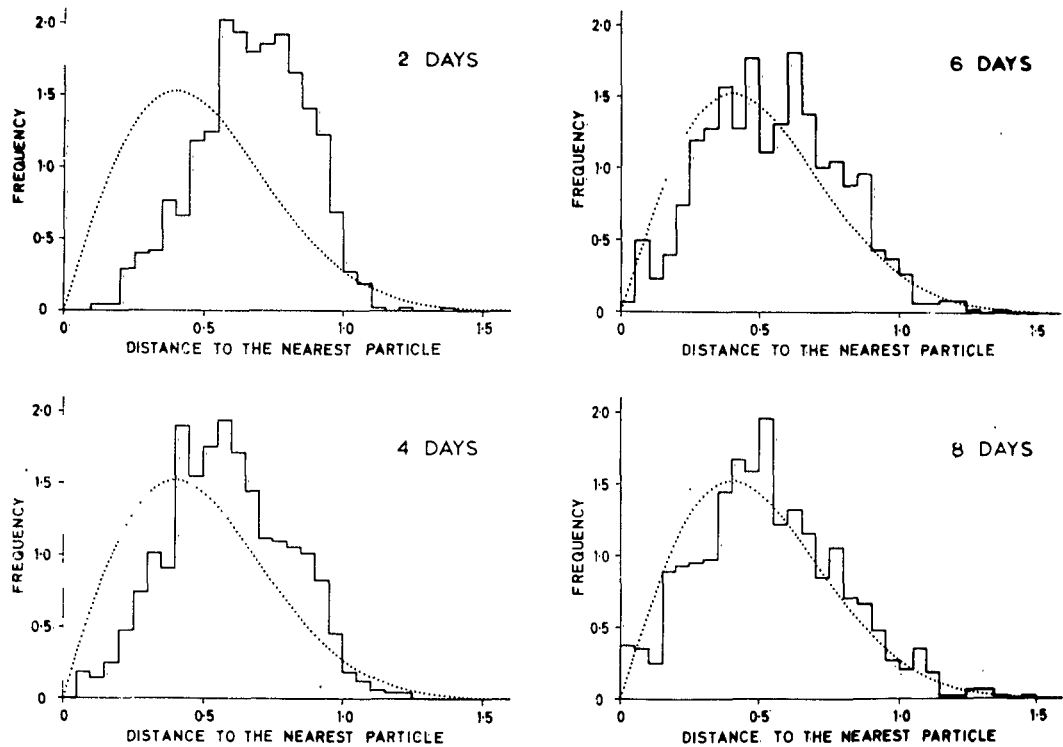


Fig. 11. Histograms of distances from each particle initially situated in a grid point to the other such particle nearest to it (full lines), and frequency curves of those distances for the case of the random distribution of particles (dotted lines). The unit of length chosen is the grid size of Fig. 1.

Acknowledgements. - The computations involved in sections on cluster expansion rates have been performed partly by Miss O. Milovanović, from the University of Belgrade, Department of Meteorology. The data concerning the zonal profiles of the mean wind and the eddy kinetic energy (Figs. 5 and 7) were evaluated and kindly made available to the author

by Dr. P. Gburčik. The program for solving the system (1) has been elaborated by the Research Section of the Deutscher Wetterdienst in Offenbach/M.

References

- Batchelor, K.G., 1950: Application of the similarity theory of turbulence to atmospheric diffusion. *Quart. J.R. Meteor. Soc.*, 76, 133-146.
- Djurić, D., 1961: On the accuracy of air trajectory computations. *J. Meteor.*, 18, 597-605.
- Durst, C.S., A.F. Crossley, and N.E. Davis, 1959: Horizontal diffusion in the atmosphere as determined by geostrophic trajectories. *J. Fluid Mech.*, 6, 401-422.
- Gifford, F., 1957a: Relative atmospheric diffusion of smoke puffs. *J. Meteor.*, 14, 410-414.
- , 1957b: Further data on relative atmospheric diffusion. *J. Meteor.* 14, 475-476.
- Hollmann, G., 1959: Transformation der Grundgleichungen der dynamischen Meteorologie in Koordinaten der stereographischen Projektion zum Zwecke der numerischen Vorhersage. *Beitr. Phys. Atmos.*, 31, 162-176.
- Mesinger, F., 1963: Remarks on the behavior of computed air trajectories near the boundaries of an octagonal area. To be published in *Beitr. Phys. Atmos.*
- Pasquill, F., 1962: *Atmospheric diffusion*. London, Van Nostrand, 297 pp.
- Phillips, N.A., 1956: The general circulation of the atmosphere: a numerical experiment. *Quart. J.R. Meteor. Soc.*, 82, 123-164.
- Welander, P., 1955: Studies on the general development of motion in a two-dimensional, ideal fluid. *Tellus*, 7, 141-156.

Monitoring Agency Document Nr.:

ASTIA Document Nr.:

REMARKS ON THE BEHAVIOUR OF COMPUTED
AIR TRAJECTORIES NEAR THE BOUNDARIES
OF AN OCTAGONAL AREA

F. Mesinger

INSTITUT FÜR METEOROLOGIE
TECHNISCHE HOCHSCHULE DARMSTADT
DARMSTADT, FED. REP. OF GERMANY

TECHNICAL NOTE NR. 3
CONTRACT NR. AF 61 (052)-366

31st OCTOBER 1962

The research reported in this document has been sponsored partly by the CAMBRIDGE RESEARCH LABORATORIES, OAR, through the European Office Aerospace Research, United States Air Force.

REMARKS ON THE BEHAVIOUR OF COMPUTED AIR TRAJECTORIES
NEAR THE BOUNDARIES OF AN OCTAGONAL AREA

F. Mesinger ⁺⁾

In the course of some investigations on atmospheric macroturbulence carried out in the Meteorological Institute of the Technische Hochschule in Darmstadt, air trajectories were computed for a period of 8 days. This computation revealed an interesting feature in the behaviour of the trajectories near the boundaries of the area. End points of the trajectories showed a tendency to accumulate in the corners of the computation area.

Trajectory computations were based on the integration of the primitive equations for the homogeneous atmosphere. Together with the continuity equation they make a complete set of equations, which in Cartesian coordinates of the distorted plane of stereographic projection [1] can be written in the form

$$\frac{\partial u}{\partial t} = m^2 (- \mathbf{v} \cdot \nabla u + \sqrt{\nabla^2 u}) - \frac{u^2 + v^2}{2} \frac{\partial m^2}{\partial x} + fv - \frac{\partial \phi}{\partial x}$$

$$\frac{\partial v}{\partial t} = m^2 (- \mathbf{v} \cdot \nabla v + \sqrt{\nabla^2 v}) - \frac{u^2 + v^2}{2} \frac{\partial m^2}{\partial y} - fu - \frac{\partial \phi}{\partial y} \quad (1)$$

$$\frac{\partial \phi}{\partial t} = - m^2 \nabla \cdot (\phi \mathbf{v})$$

In (1) $\mathbf{v}(u,v)$ is the "reduced image velocity" [1], while other symbols have their usual meaning. The system (1) was solved with the aid of a program for the computer IBM 704

⁺⁾ On leave from the University of Beograd, Meteorological Department

elaborated by the Research Section of the German Weather Service. As the boundary conditions the values $\psi(t) = 0$ at all the boundary grid points were prescribed. The initial wind field was obtained from the field of geopotential by solving the balance equation. The forecast covered an octagonal area, centered on the North Pole and extended southward to about 10°N latitude.

The program for the solution of system (1) had the wind components in all grid points and at desired time intervals as an output. Trajectories for a period of 8 days were computed for all the 2080 grid points, with the use of those wind components at time intervals of 30 minutes. The computation was made with centered time and space differences. To the viscosity coefficient ν in (1) the value of $0.517 \cdot 10^9 \text{ cm}^2 \text{ sec}^{-1}$ was prescribed. The computation was started with the geopotential field of the 500 mb surface for the 26 August 1958, 00 GMT.

An examination of the end points of the 8-days trajectories (Fig. 1) showed an interesting feature concerning the spacing of points in some corners of the area. Let us consider the four rows of grid points adjacent to the boundaries of the area and parallel to the sides of the figure. At three out of these four rows the end points of the trajectories, which started in the grid points, moved westward along the rows and accumulated at their ends. Moreover, these rows acted as traps for the points which reached them from the interior of the area. Fairly large regions without points appeared due to this inability of points to leave those rows.

Such behaviour of the trajectories appeared as a consequence of the fact that at these four rows the velocity components normal to the boundary were extremely small during the whole period of the forecast. In the beginning these normal velocity components were equal to zero: since the initial wind field was obtained by the use of the stream function, and both velocity components had to be zero at the boundary points, a constant value had to be prescribed

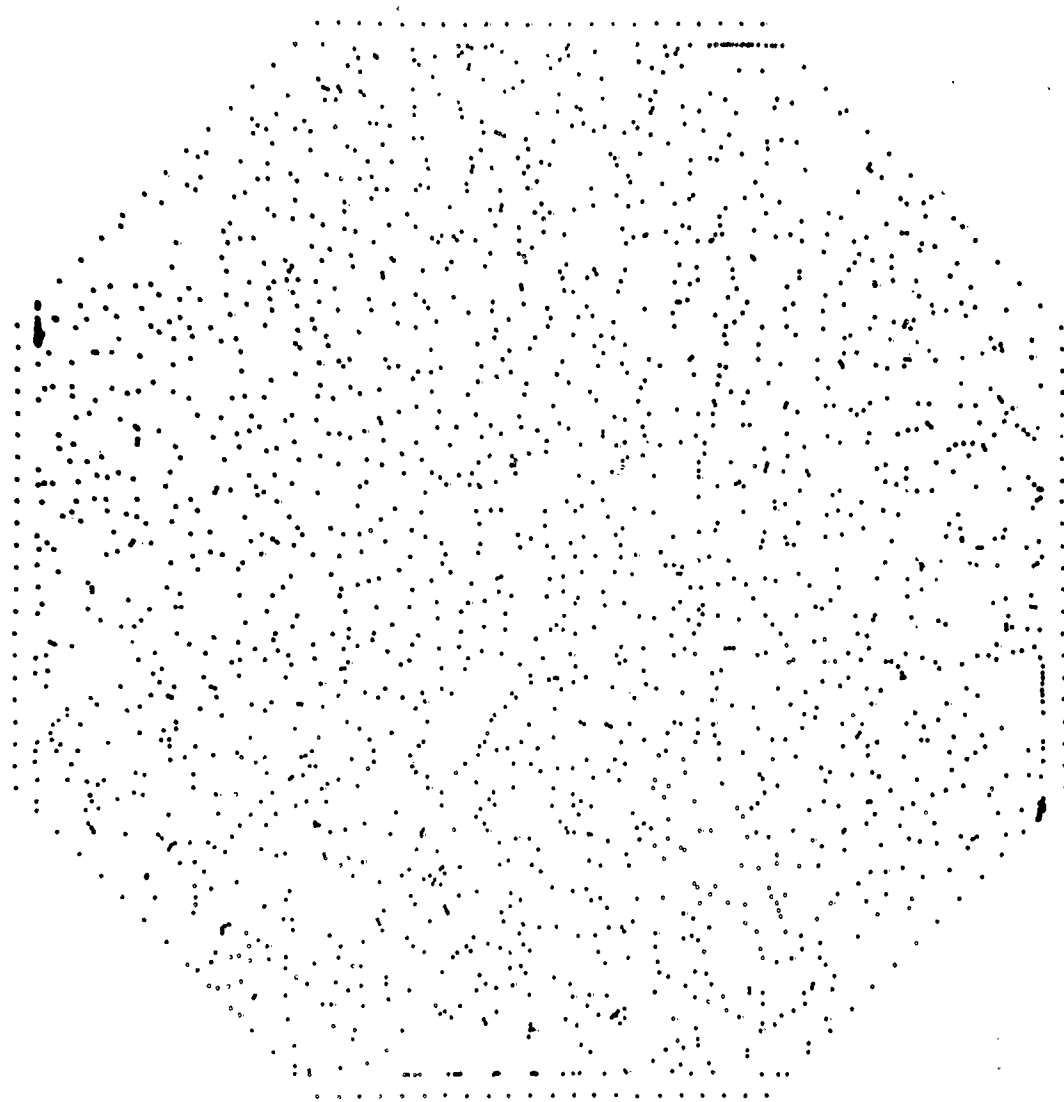


Fig.1. End points of the 8-days trajectories which originated in the grid points

to the stream function at the boundary points and the points adjacent to the boundary. As a consequence the velocity compo-

nents normal to the boundary were also zero at the four considered rows adjacent to the boundary. During the first two days of the forecast these normal velocity components increased only to about 0.2 m sec^{-1} ; after that time they remained at this small order of magnitude.

The accumulation and depletion of the trajectory points is likely to be accompanied with the mass accumulation and depletion. Numerical instability which appears always after a certain time at the boundaries of the computation area could be a consequence of this mass accumulation and depletion.

Acknowledgement: The program for solving the system (1) has been elaborated by the Research Section of the Deutscher Wetterdienst in Offenbach/M.

Reference

1. G. Hollmann, Transformation der Grundgleichungen der dynamischen Meteorologie in Koordinaten der stereographischen Projektion zum Zwecke der numerischen Vorhersage. Beitr. Phys. Atmos. 31 (1959) 162 - 176.